Translational Oncology 25 (2022) 101516

Contents lists available at ScienceDirect

Translational Oncology

journal homepage: www.elsevier.com/locate/tranon

Original Research

Anlotinib exerts potent antileukemic activities in Ph chromosome negative and positive B-cell acute lymphoblastic leukemia via perturbation of PI3K/AKT/mTOR pathway

Qiuling Chen [a,b,c], Qian Lai [a,b,†], Yuelong Jiang [a,b,†], jingwei Yao [a,b], Qinwei Chen [a,b], Li Zhang [a,b], Caiyan Wang [a,b], Yong Zhou [a,b,*], Manman Deng [a,b,*], Bing Xu [a,b,*]

[a] Department of Hematology, The First Affiliated Hospital of Xiamen University and Institute of Hematology, School of Medicine, Xiamen University, No.55, Zhenhai Road, Siming District, Xiamen, Fujian 361003, China
[b] Key Laboratory of Xiamen for Diagnosis and Treatment of Hematological Malignancy, Xiamen 361102, China
[c] Department of Hematology & Oncology, Fujian Children's Hospital, Fujian Branch of Shanghai Children's Medical Center, Fuzhou 350000, China

ARTICLE INFO

Keywords:
Acute lymphoblastic leukemia (ALL)
Anlotinib
VEGF/VEGFR2
PI3K/AKT/mTOR
Tyrosine kinase inhibitor (TKI)

ABSTRACT

Objectives: Despite advances in the development of novel targeted therapies, the need for B-ALL alternative treatments has not been met. Anlotinib could blunt the proangiogenic activity of VEGFR, PDGFR, and FGFR, and has shown strong antitumor activities across multiple tumors. However, anlotinib cytotoxicity against B-ALL has not ever been evaluated, thus prompting us to initiate this study.

Methods: Expression2Kinases program was used to identify potential treatment targets. Cell viability and apoptosis were determined by CCK-8 and Annexin V/PI staining kit, respectively. qRT-PCR and Western blotting were utilized to investigate the molecular mechanisms. *In vivo* antileukemia activity of Anlotinib was evaluated in a Ph^+ B-ALL patient-Derived Xenograft (PDX) model.

Results: Compared with treatment-naive B-ALL cases, RR B-ALL patients had higher activities in the VEGF/VEGFR signaling and the PI3K/AKT/mTOR pathway. Exposure of Ph^- and Ph^+ B-ALL cells to anlotinib resulted in significant cell viability reduction, apoptosis enhancement, and cell cycle arrest at G2/M phase. Importantly, anlotinib treatment led to remarkably decreased leukemia burdens and extended the survival period in a Ph^+ B-ALL PDX model. Blockade of the role of the proangiogenic mediators, comprising VEGFR2, PDGFR-beta, and FGFR3, played a critical role in the cytotoxicity of anlotinib against Ph^- and Ph^+ B-ALL. Moreover, anlotinib dampened the activity of PI3K/AKT/mTOR pathway that resides in the convergence of the three mentioned proangiogenic signals.

Conclusion: This work provides impressive preclinical evidence of anlotinib against Ph^- and Ph^+ B-ALL and raises a rationale for future clinical evaluation of this drug in the management of Ph^- and Ph^+ B-ALL.

Introduction

Acute lymphoblastic leukemia (ALL) is a heterogeneous hematopoietic malignancy originated from malignant transformation and uncontrollably clonal proliferation of B- or T-lineage lymphoid precursor cells [1]. Precursor B-cell derived ALL (B-ALL) is the most frequent immunological subtype, accounting for around 80% of all newly diagnosed ALL cases. In general, B-ALL can be stratified into Ph^- and Ph^+ subtypes based on whether it carries a reciprocal translocation (t) between chromosomes 9 and 22 (t[9,22][q34;q11]), with the latter group

Abbreviations: ALL, B-cell acute lymphoblastic leukemia; RR AB-ALL, refractory/relapsed B-ALL; TKI, tyrosine kinase inhibitor; RTK, receptor tyrosine kinase; PDX, patient-derived xenograft; CCK-8, cell counting kit-8; qRT-PCR, quantitative real-time polymerase chain reaction; NSCLC, non-small-cell lung cancer; CAR-T, chimeric-antigen receptor (CAR)-modified autologous T cells; GEO, gene expression omnibus; DEGs, differentially expressed genes; FDR, false discovery rate; FC, fold-change; GO, gene ontology analysis; KEGG, kyoto encyclopedia of genes and genomes; CFDA, China's Food and Drug Administration.

* Corresponding authors at: Department of Hematology, The First Affiliated Hospital of Xiamen University and Institute of Hematology, School of Medicine, Xiamen University, No.55, Zhenhai Road, Siming District, Xiamen, Fujian 361003, China.
E-mail addresses: hexianxiaozi@163.com (Y. Zhou), marina_deng@outlook.com (M. Deng), xubing@xmu.edu.cn (B. Xu).
† These authors contributed equally to this work.

https://doi.org/10.1016/j.tranon.2022.101516
Received 23 May 2022; Received in revised form 21 July 2022; Accepted 9 August 2022

having worse prognosis than the former one [2]. Owing to the advancements of currently multiagent intensive chemotherapies, curative rates achieve in around 90% of children with B-ALL [3,4], while less than 50% of B-ALL in adults experience long-term survival [5]. Clinical outcomes for relapsed and chemotherapy-refractory disease (RR B-ALL) remain worse [6]. New emergent therapeutic approaches, including the bispecific T-cell engager such as Blinatumomab and CD19-specific chimeric antigen receptor (CAR) modified autologous T cells (CAR-T) treatment, have considerably changed the clincial courses of patients with RR B-ALL [7,8]. However, failure to or losing an initial response to these novel strategies often occurs [9], suggesting that exploring alternative high-efficient treatment options is still an unmet medical need for the treatment of patients with RR-B-ALL.

Angiogenesis is a process of fresh blood vessel formation from a preexisting vascular network. This process is under exquisite control of many proangiogenic and antiangiogenic factors [10,11]. During malignant transformation, the angiogenesis-associated signals are deregulated with multiple proangiogenic factors being upregulated and thus tilting toward the proangiogenic switch [12]. VEGF, PDGF, and FGF are three main proangiogenic components and exert their functions predominantly through binding to their corresponding receptors, VEGFR, FGFR and PDGFR, respectively [13,14]. Given the pivotal functions of angiogenesis in diverse cancer initiation and development, including ALL, various antiangiogenic therapeutics have been developed and some of them have moved forward to clinical evaluation in multiple cancer types [15]. Nevertheless, the angiogenesis-blocking approaches show moderate antitumoral effects, probably attributable to the fact that they are incapable of fully disrupting these different proangiogenic signals [14,16]. This provides an opportunity for multitarget antiangiogenic agents as a promising anticancer strategy. Antivascular therapies have demonstrated impressive antitumoral activities in many cancers, while their effects on B-ALL have been poorly studied. Previous reports have found that ALL patients upregulates the expressions of some important VEGF receptors (VEGFRs), such as VEGFR1 and VEGFR2, and the upregulation of these VEGFRs was associated with poor clinical outcomes [17,18]. More importantly, antivascular drugs including anti-VEGFR agents have demonstrated promising antileukemia activity in ALL [19].

Anlotinib is a newly developed oral receptor tyrosine kinase (RTK) inhibitor that primarily targets VEGFR, FGFR, and PDGFR, three critical receptors of proangiogenic factors [20]. Owing to its encouraging clinical outcome and manageable safety profiles, anlotinib has been approved in China as a third-line treatment for patients with advanced or metastatic non-small-cell lung cancer (NSCLC) who have experienced disease progression or recurrence [21–23]. In addition, numerous phase II/III clinical trials have been launched to evaluate the antitumoral activity of anlotinib against other malignancies, including gastric cancer, hepatocellular carcinoma and renal carcinoma. These trials have preliminarily demonstrated that anlotinib administration led to clinical benefits in cancer patients [24–26]. Despite the excellent antitumoral activity of anlotinib in multiple forms of solid tumors, the antileukemia efficacy of anlotinib in B-ALL remains to be defined. This prompts us to investigate the cytotoxic effects of anlotinib on B-ALL and its underlying mechanism of action.

Methods and materials

Data acquisition

Gene array data were screened using the Gene Expression Omnibus (GEO; http://www.ncbi.nlm.nih.gov/geo) database. Human B-ALL expression profile dataset GSE60926 was downloaded from GEO. The GSE60926 dataset contains 22 B-ALL bone marrow samples at diagnosis, 20 bone marrow samples at relapse, and 8 cerebrospinal fluid (CSF) samples at relapse. The dataset was analyzed using the GPL570 Affymetrix Human Genome U133 Plus 2.0 Array platform. For result verification, raw counts of RNA-sequencing data and corresponding clinical information from 135 ALL samples were obtained from Therapeutically Applicable Research To Generate Effective Treatments (TARGET) dataset (https://ocg.cancer.gov/programs/target), in which the method of acquisition and application complied with the guidelines and policies.

Differentially expressed genes (DEGs) identification, downstream pathway enrichment, and upstream kinase enrichment analysis

The raw data of GSE60926 in the CEL file was effectively processed using the Affy package pair in R, using correction, normalization and log2 conversion [27]. Absent probes were filtered. The duplicate probes were merged by the maximum value and processed for probe annotation using "hgu133plus2.db" R package. The DEGs in B-ALL relapse samples compared with the samples at diagnosis were determined using limma package [28]. DEGs were screened with a false discovery rate (FDR) corrected $P<0.05$ and $|\log \text{fold change (FC)}|>1$. Functional enrichment for downstream pathways was performed by the web-based genomic annotation tool: DAVID (https://david.ncifcrf.gov/) [29]. DEGs were subjected to molecular function and pathway studies by Gene Ontology (GO) analysis and Kyoto Encyclopedia of Genes and Genomes (KEGG) pathway analysis. DEGs were also used to predict upstream regulatory kinases by web-based Expression2Kinases software [30]. Sankey diagrams were generated by the ggalluvial R package. The KM survival analysis with log-rank test were also used to compare the survival difference between above two groups or more groups. TimeROC analysis was performed to compare the predictive accuracy of each gene and risk score. For Kaplan–Meier curves, *p*-values and hazard ratio (HR) with 95% confidence interval (CI) were generated by log-rank tests and univariate Cox proportional hazards regression. All analytical methods above and R packages were performed using R software version v4.0.3 (The R Foundation for Statistical Computing, 2020). $p < 0.05$ was considered as statistically significant.

Cell lines and reagents

Ph^-B-ALL Nalm6 and Ph^+B-ALL SupB15 cells were kept in our lab and routinely cultured in RPMI 1640 medium (Invitrogen, Life Technologies, Carlsbad, California, USA) supplemented with 10% fetal bovine serum and 100 units/ml penicillin and 100 mg/ml streptoMYCin at 37°C in a humidified 5% CO2 incubator. Anlotinib, a kind gift provided by Zhengda Tianqing Pharmaceutical Group Co., Ltd, was dissolved in dimethyl sulfoxide (Sigma, St Louis, MO, USA) at a stock concentration of 100 mM and diluted with culture median to designated concentrations. KI8751, a selective VEGFR2 inhibitor,\ was dissolved in dimethyl sulfoxide (Selleckchem, TX, USA). The concentrations of anlotinib in the following assays were referenced to prior reports demonstrating the efficacy of anlotinib in solid tumors and was determined by our previous laboratory experience in AML and the preliminary results of the cytotoxicity of anlotinib against B-ALL cells [31].

Cell viability assay

Cell viability of Nalm6 and SupB15 cells treated with Anlotinib or KI8751 was determined by a Cell Counting Kit-8 (CCK-8; Dojindo, Kumamoto, Japan) assay. In brief, B-ALL Cells (5×10^4 cells/well) suspended in 100 μl growth medium were seeded in 96-well plates and immediately treated with designated doses of Anlotinib for 24 and 48 h. At the end of the treatment, CCK-8 reagents (10 μl/well) were added and continued to incubate for an additional 2 h, after which the absorbances were detected at 450 nm by a microplate reader (ELx800; BioTek Instruments Inc., Winooski, Vermont, USA). Cell viability was calculated with the following formula: cell viability rate (%) = (absorbance of experimental group − absorbance of blank well) / (absorbance of control group- absorbance of blank well) × 100%. The IC50 value of each

cell line was calculated based on the results of cell viability. The data was obtained from three independent experiments in triplicate, and presented as mean ± S.D.

Apoptosis and cell cycle analysis

Nalm6 and SupB15 cells were exposed to different concentrations of Anlotinib (0, 1, 2, 4, and 8 μM) or KI8751 (0, 0.1, 1, 1.5, 2 nM) for 24 h or 48 h. Anlotinib-treated cells were then stained with Annexin V/PI staining kit (eBioscience, San Diego, California, USA) per the manufacturer's instructions. The stained cells were analyzed by flow cytometry (FACS Caliber; BD Biosciences, San Jose, California, USA). Apoptotic cells were defined as Annexin-V positive cells.

For cell cycle assessment, 2×10^5 of either Nalm6 or SupB15 cells were exposed to Anlotinib (0, 2, 4, 8 μM) or KI8751 (0, 0.1, 1, 1.5, 2 nM) for 24 h. Subsequently, Anlotinib-exposed cells were stained with PI/RNase staining buffer and then referred to flow cytometer analysis (BD Biosciences, San Jose, California, USA), following the manufacturer's instructions. Both assays were performed in independent triplicates for three times.

B-ALL patient derived xenograft (PDX) animal model

NOD-Prkdc−/−IL2rg−/- mice (male, NPI, IDMO ltd., Beijing, China) were housed under specific-pathogen-free (SPF) environment in accordance with the animal care guidelines of Xiamen University Animal Care and Use Committees. In this study, each mouse was intravenously engrafted with 1×10^6 of Ph^+ B-ALL cells from a primary PDX B-ALL mouse tissue within 24 h of receiving 1 Gy of irradiation. Once detecting human CD45 staining (clone HI30, Biolegend) in peripheral blood $\geq 1\%$, a total of 22 PDX mice were randomized to control the or Anlotinib group (5 mg/kg, 5-day on and 2-day off) for three-week treatment. At the end of treatment, 5 PDX mice from each group were euthanized and used to evaluate the antileukemia efficacy of anlotinib in a B-ALL preclinical model. The remaining 6 mice of both groups were utilized to determine the survival curve. During the treatment course, the body weight of each mouse was monitored daily to assess the toxicity profiles of anlotinib for the treatment of B-ALL in a preclinical model.

Western blotting and quantitative real-time polymerase chain reaction (qRT-PCR) analysis

Nalm6 and SupB15 cells (5×10^6/ml) were cultured with Anlotinib (0, 2, 4, 8 μM) for 24 h. At the end of treatment, cells were harvested and lysed in RIPA buffer (Thermo Scientific, USA) supplemented with protease inhibitors (Roche Diagnostics, Mannheim, Germany) and phosphatase inhibitors (Roche Diagnostics, Mannheim, Germany). Protein concentrations were quantified and normalized by a BCA protein Assay (Pierce, Thermo Scientific, USA). Equal protein concentrations of each treatment group (20 μg/lane) were electrophoresed on 8 to 12% gels and then transferred to PVDF membranes (Millipore, Billerica, MA, USA). The membrane was probed with primary antibodies and HRP-conjugated secondary antibodies (all from Cell Signaling Technology, Danvers, MA, USA). Ultimately, an ECL Western Blotting Detection Kit (GE Healthcare, Chicago, USA) was used to detect the protein signals that were visualized by the Amersham Imager 600 (AI600, GE Healthcare, Chicago, USA).

Total RNA was extracted from cultured cells using TRIzol reagent (Invitrogen, USA). It was reverse transcribed into cDNA using the PrimeScript RT kit (Takara, Japan) according to the manufacturer's instructions. The cycling conditions were 95 °C for 10 s, 60 °C for 20 s, and 72 °C for 20 s. Each reaction was repeated three times. The primer sequences for RT-PCR are shown in Table S1.

Statistical analysis

Statistical analyses were performed with IBM SPSS 19.0 software (SPSS, Chicago, IL) and GraphPad Prism 8 (GraphPad Software Inc, San Diego, CA, USA). The results for continuous variables were presented as mean ± standard deviation values. Student's t test or Wilcoxon signed-rank test were used for between-group comparisons. Categorical data were analyzed using chi-square tests or Fisher's exact test. *P* values < 0.05 (two-tailed) were considered to indicate statistically significant results. All triplicate results were quantification of independent experiments.

Results

In silico analysis predicts anlotinib as a potential anti-leukemic therapeutic regimen in patients with B-ALL

To discover new fundamental pathways and cellular biomarkers that might be crucial for B-ALL, we harbored a published B-ALL microarray data (GSE60926) on 40 B-ALL bone marrow samples at diagnosis (n=20) or at relapse (n=20) from Gene Expression Omnibus (GEO) database. Raw data was directly downloaded from the GEO database. Quality control and background normalization were performed with the "affy" R package [27]. After excluding the absent probes, 39177 and 39008 normalized probes were separately observed in newly diagnosed and relapsed B-ALL samples. Next, we merged the duplicate probes by the maximum value and processed the remaining probes for probe annotation by "hgu133plus2.db" R package. "Limma" R package was employed to determine differential expression genes (DEGs) between the newly diagnosed and relapsed groups. In the end, the two groups exhibited a different expression pattern, manifested by a clustered expression heatmap, which was generated by the DEGs with a cutoff value of $|\text{fold change (FC)}| > 1$ (Fig. 1A). Importantly, we identified 27 downregulated genes and 64 upregulated genes (Fig. 1B).

To uncover novel potential pathways regulated by these DEGs in B-ALL, we performed Gene Ontology (GO) enrichment analysis with KEGG pathway database [32]. Consequently, several significant affected pathways, including VEGF signaling cascade, were selected and shown in a bar graph (Fig. 1C). VEGF signaling pathway, an angiogenesis-associated pathway, was also enriched by significant DEGs. PI3K/Akt signaling pathway, which has been implicated in both the pathogenesis and progression of leukemia was also highlighted [33]. To rule out the selection bias of the analyzing dataset, we acquired 135 ALL RNA-seq data as the verification cohort. Key regulatory genes from PI3K/Akt signaling pathway were used as the potential survival markers to predict the overall survival rate in verification cohort. All the key regulatory genes were able to predict the ALL survival rate with the same trend (Fig. S1A-C). So the PI3K/Akt signaling pathway might be the potential therapeutic marker in B-ALL.

Knowing that upstream receptor tyrosine kinase can cause the change of the downstream gene expression profile [34,35]. We applied "Expression2Kinases" to identify the upstream kinases of the DEGs. Upstream kinases like AKT1, CDK1, FGFR1, RET, and so on were combined with enriched pathways using Sankey diagram to emphasize the potential regulatory kinase in relapse B-ALL (Fig. 1D). Protein kinase inhibitors were gaining increasingly attention in leukemia therapies [36] and also relapsed B-ALL[37]. Next, we combined China's Food and Drug Administration (CFDA) approved TKIs, their potential target kinases, downstream regulatory pathways, and their corresponding relationships in the Sankey diagram (Fig. 1E). Venn diagram showed the overlapped kinases (Fig. 1F) and downstream enriched pathways (Fig. 1G). RET and ALK were shown in the overlapped kinase diagram (Fig. 1F), and Pi3K-AKT signaling pathway, VEGF signaling pathway, MAPK signaling pathway, and cell cycle pathway were shown in the overlapped pathway diagram (Fig. 1G). Anlotinib was proven to target RET kinase and downstream pathways like Pi3K-AKT signaling pathway

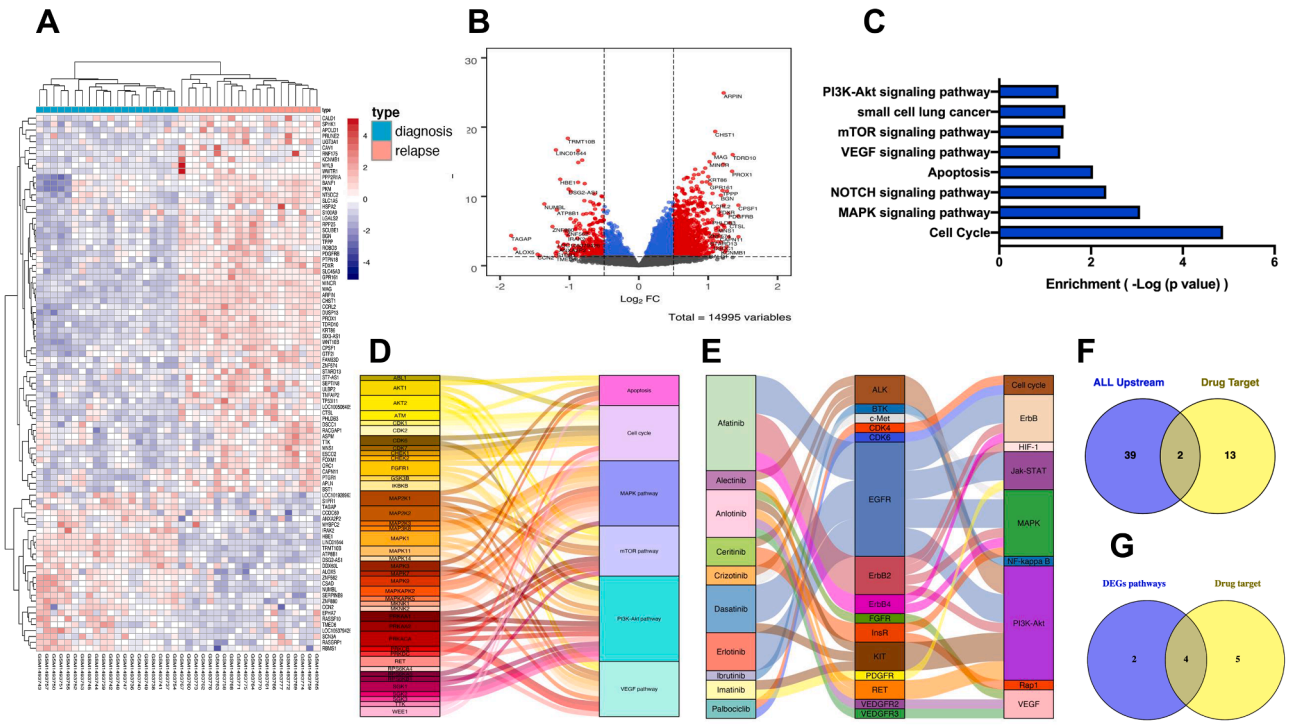

Fig. 1. In silico analysis predicted anlotinib as a potential anti-leukemic therapeutic choice. (A) & (B) Clustered heatmap and volcano plots were generated by the normalized and annotated significant differential expressed genes (corrected P<0.05 and |log fold change (FC)|>1). (C) GO analysis of DEGs whose expression was altered in relapsed B-ALL cases. (D) Potential upstream regulatory kinase and downstream enriched pathway network was constructed by DEGs. (E) TKI-Kinase-Pathway network was constructed and shown. (F) & (G) Potential upstream kinase and potential downstream pathways were suggested by the overlapped section.

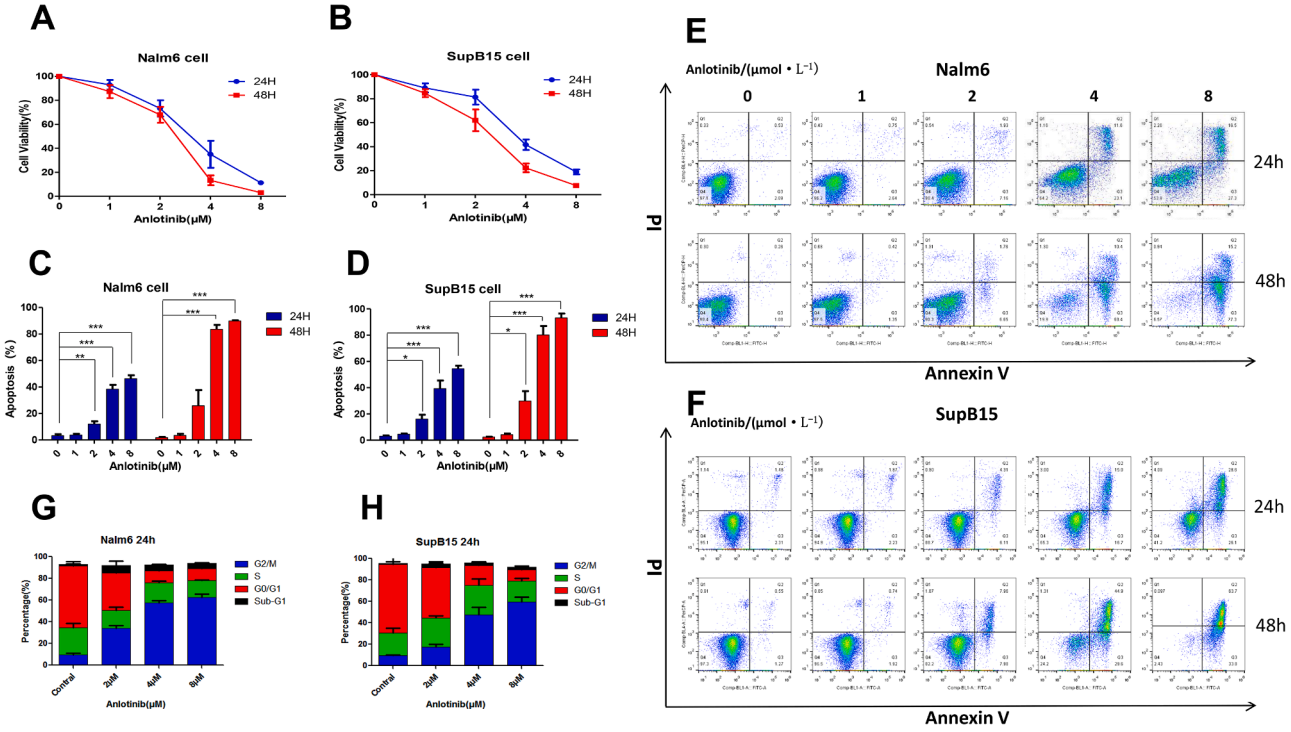

Fig. 2. The cytotoxic effects of anlotinib on Ph^- and Ph^+ B-ALL cells. (A) & (B) Exposure of either Nalm6 or SupB15 cells to designated concentrations of anlotinib for 24 and 48h, cell viability was determined with a CCK-8 kit. (C) & (D) Flow cytometric analysis of cell cycle distribution of Nalm6 or SupB15 cells treated with distinct concentrations of anlotinib for 24h. (E-F) Annexin V/PI dual-staining assay was used to analyze the cell apoptotic proportions of Nalm6 and SupB15 cells treated with or without anlotinib for 24 and 48 h. (G-H) Representative flow cytometric plots of Nalm6 or SupB15 cells exposed to indicated doses of anlotinib for 24 and 48h. Each experiment was independently performed three times in triplicate. *$P < 0.05$, **$P < 0.01$, ***$P < 0.001$.

and VEGF signaling pathway (Fig. 1E) [38]. Taken together, our bioinformatic analyses point out that anlotinib might be a potential therapeutic regimen in B-ALL treatment.

Anlotinib attenuates cell viability, blocks cell cycle at G2/M phase, and induces apoptosis in Ph−and Ph+ B-ALL cells

In this study, Nalm6 and SupB15 cells were used as Ph^- and Ph^+ B-ALL *in vitro* models, respectively. To investigate the antileukemic effect of anlotinib on Ph^- and Ph^+ B-ALL, Nalm6 and SupB15 cell lines were cultured with or without anlotinib (1, 2, 4, and 8 μM) for 24 and 48 h, respectively. Cell viability was determined by a CCK8 assay and cell apoptosis was evaluated with an annexin V/PI dual-staining assay. Compared with the untreated group, anlotinib treatment significantly decreased the viability of Ph^- and Ph^+ B-ALL cells in dose- and time-dependent manners (Fig. 2A and B). The IC50 values of anlotinib after 24-h treatment were 3.224 ± 0.875 μM and 3.803 ± 0.409 μM in Nalm6 and SupB15 cells, respectively. For 48-h treatment, the IC50 values of anlotinib for Nalm6 and SupB15 cells were 2.468 ± 0.378 μM and 2.459 ± 0.443 μM, respectively (Table 1). As expected, exposure of Nalm6 and SupB15 cells to anlotinib remarkably increased cell apoptosis, including both early and late apoptosis in dose- and time-dependent fashions (Fig. 2C–F).

Next, we assessed the cell cycle distribution of both Nalm6 and SupB15 cells treated with or without anlotinib (2, 4, 8 μM). Here, treatment of Nalm6 cells with anlotinib clearly increased the percentage of G2/M phase, and simultaneously decreased the percentage of G1/G0 phase (Fig. 2E). Accordingly, similar results of the cell cycle distribution were also observed in the SupB15 cells treated with or without anlotinib (Fig. 2F). Altogether, these findings demonstrated that anlotinib exerted potent antileukemic activity in both Ph^- and Ph^+ B-ALL cell lines through suppression of cell viability, induction of apoptosis, and blockade of cell cycle.

In addition, another selective VEGFR2 antagonist KI8751 was employed to confirm the findings of anlotinib as an angiogenic blocker against B-ALL cells. We treated Nalm6 and SupB15 cell lines with a series of KI8751 for 24 and 48 h. Similar to the antileukemic activity of anlotinib in B-ALL cells, KI8751 treatment was potent to induce loss of both Nalm6 and SupB15 cell viabilities in dose-dependent and time-dependent manners (Fig. S2A and B). KI8751 exposure had proapoptotic capability in Nalm6 (Fig. S2C, upper panel and 2D) and SupB15 cells (Fig. S2C, bottom panel and 2D) in dose-dependent fashion. As anticipated, cell cycle of KI8751 treated Nalm6 and SupB15 cells was accumulated at G0/G1 phase with the percentage reduction of S phase (**Fig. S2F** and **G**).

Anlotinib abrogates leukemic cell growth in a patient-derived xenograft (PDX) B-ALL mouse model

To further consolidate the robust anti-B-ALL efficacy of anlotinib *in vivo*, we reestablished a PDX model by intravenously engrafting 1×10^6 of Ph^+ B-ALL cells obtained from a primary PDX B-ALL mouse tissue into *NOD-scid IL2Rγ* ^{null} (NSG) mice (**Fig. 3A**). Upon detecting a human CD45 percentage of >1% in the peripheral blood, Ph^+ B-ALL PDX mice were randomized into either vehicle (n=11) or anlotinib treatment group (n=11). Anlotinib (5 mg/kg/d) was orally administered from Monday to Friday (5 days on, 2 days off) for 3 consecutive weeks (**Fig. 3A**). Body weight of each mouse was measured for 5 days per week during the entire treatment course. In comparison with the untreated group, anlotinib administration appeared to moderately increase mice body weight (**Fig. 3B**), indicating that anlotinib is well tolerated in the treatment of B-ALL preclinical models. In addition, no other treatment relevant safety profiles had been noticed in the anlotinib group versus the vehicle group. These observations were in concert with the fact that anlotinib was active against multiple malignant diseases and had acceptable adverse effects in a series of clinical trials.

At the end of the experiment, 5 out of 11 PDX mice from each group were randomly selected and then euthanized to evaluate the antileukemic activity of anlotinib. The remaining mice in each group continued to be housed and utilized to analyze the survival curve. Administration of Ph^+ B-ALL PDX mice with anlotinib significantly reduced the size and weight of spleen when compared with the anlotinib-untreated group (Fig. 3C and D). More notably, anlotinib remarkably attenuated the leukemia burden in both bone marrow and spleen, as evidenced by substantial decreases of human CD45 and CD19 positive cells (Fig. 3E–H). In contrast to the control group, anlotinib treatment strikingly prolonged the survival period of the Ph^+ B-ALL PDX mice (Fig. 3I). Taken together, the *in vivo* data revealed that anlotinib showed robustly antitumoral effects on B-ALL models with neglectable safety profiles.

Anlotinib decreases the levels of key proangiogenic factor receptors and perturbs the activity of the PI3K/AKT/mTOR signaling pathway in Ph− and Ph+ B-ALL cells

Anlotinib is designed to predominantly target VEGFR, PDGFR, and FGFR which play important roles in angiogenesis. Not surprisingly, we found anlotinib significantly diminished the mRNA expression levels of VEGFR2, PDGFR-beta, and FGFR3 in Ph^- and Ph^+ B-ALL cells (Fig. 4A and B).

Our bioinformatic results revealed that perturbation of the PI3K/AKT signaling cascade might contribute to the cytotoxicity of anlotinib against B-ALL (Fig. 1G). This observation drove us to examine whether it still held true in our cellular models. As expected, exposure of Ph^- and Ph^+ B-ALL cells with anlotinib downregulated the enrichment of the phosphorylation of several crucial components of this pathway, including PI3K, AKT, and mTOR (Fig. 4C). Altogether, these results suggested that anlotinib exhibited its effective anti-leukemia activity in Ph^- and Ph^+ B-ALL cells, primarily through attenuation of three key proangiogenic mediators and decrease of the function of the PI3K/AKT signaling pathway.

Table 1
The IC50 values of Nalm6 and Sup15 cells treated with Anlotinib for 24 and 48 h.

Cell lines	IC50 ± S.D (μmol/L)	
	24 h	48 h
Nalm6	3.224 ± 0.875	2.468 ± 0.378
Sup15	3.803 ± 0.409	2.459 ± 0.443

Discussion

In this study, we demonstrated that patients with RR B-ALL had a distinct gene expression signature compared to patients with newly diagnosed B-ALL. This signature included a significant upregulation of the proangiogenic VEGF/VEGFR signaling and its downstream PI3K/AKT pathway in RR B-ALL. The observation indicates that the proangiogenic signal might be important for the development of RR B-ALL and could be a potential therapeutic target for the treatment of this malignant entity. VEGF, a well-known proangiogenic factor, plays a crucial role in angiogenesis through binding to its receptors (VEGFs) which consist of VEGFR-1, VEGFR-2, and VEGFR-3. Among these receptors, VEGFR-2 is regarded as the main receptor to transmit the proangiogenic signal [13]. Blocking the VEGF/VEGFR signaling as an antitumor strategy has been extensively investigated over the past decades, and some investigations have shown that attenuation of this signaling resulted in modest or significant antitumor effects [19]. Therefore, several anti-VEGF/VEGFR strategies have been approved for the treatment of numerous solid tumors, encompassing metastatic colorectal cancer, hepatocellular carcinoma, non-small-cell lung cancer (NSCLC), and renal cell carcinoma, etc. [39]. However, therapeutic resistance to the anti-VEGF/VEGFR treatment approaches often occurs and correlates

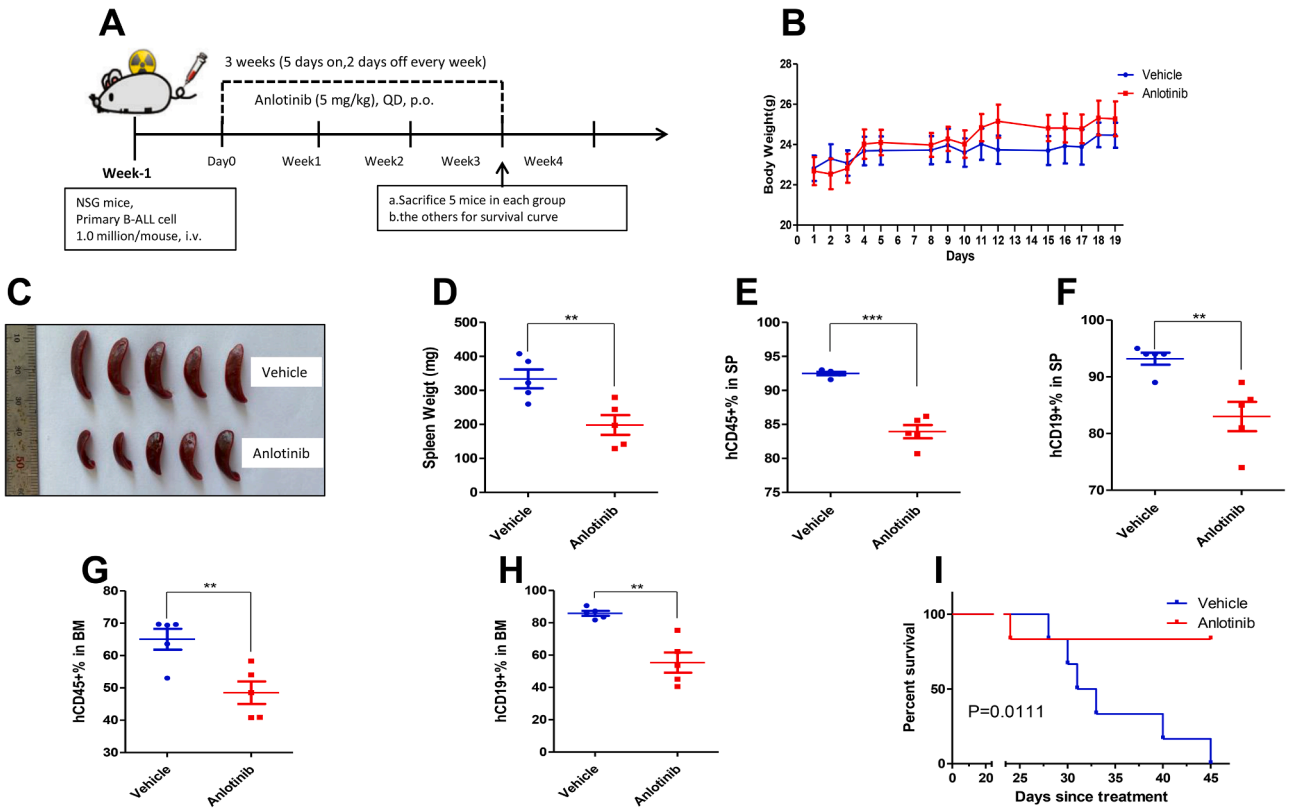

Fig. 3. Anlotinib reduces leukemic burden and prolongs survival in a patient-derived xenograft (PDX) Ph^+ B-ALL mouse model. (A) The scheme for the timeline of the experiments using a PDX mouse model. (B) Monitoring of body weight once daily in both vehicle and anlotinib groups during the entire treatment course. Each point represents the mean ± S.D. for body weight in each group. (C) & (D) The size and weight of the spleen were measured in each group. (E-H) Flow-cytometric analysis of the percentage of human $CD45^+$ and human $CD19^+$ leukemic cells in spleen and femur bone marrow. (I) Assessment of Kaplan–Meier survival curve in control and anlotinib groups.

with poor outcomes [40]. Treatment failure to the anti-VEGF/VEGFR regimen is possibly due to the activation of alternative proangiogenic signals, incorporating the PDGF/PDGFR pathway and the FGF/FGFR pathway [41]. This suggests that simultaneously targeting the VEGF/-VEGFR, the PDGF/PDGFR, and the FGF/FGFR pathways might be a more potential potent treatment option than solely inhibiting the VEGF/VEGFR signaling.

Anlotinib is developed to abrogate the activity of angiogenesis via inhibition of the proangiogenic functions of VEGFR, PDGFR, and FGFR [20]. Previous studies demonstrated that anlotinib was potent to decrease cell viability and promote cell apoptosis in dozens of solid tumor preclinical models [21–23]. In phase I/II clinical trials, anlotinib treatment resulted in encouraging clinical responses in patients with recurrent solid tumor, manifested by a significantly increased overall response rate and prolonged median overall survival [24–26]. Owing to these promising results, this drug has received an approval from the Chinese Food and Drug administration (CFDA) to treat recurrent NSCLC patients [23]. Our prior work revealed that this agent was cytotoxic to MLL-rearranged acute myeloid leukemia via suppression of SETD1A/AKT-mediated DNA damage response [31]. Nevertheless, there has limited study evaluating the cytotoxic effects of anlotinib on ALL. In the present study, *in vitro* preclinical models illustrated that treatment of both Ph^- and Ph^+ B-ALL cells with anlotinib markedly diminished cell viability, triggered apoptotic cell death, and enriched cell cycle in G2/M phase. Furthermore, oral administration with anlotinib considerably abrogated the leukemia burden in bone marrow and spleen, and extended the survival period in a PDX model engrafted with patient-derived Ph^+ B-ALL cells. Consistent with its favorable adverse effects reported in other studies, no unacceptable side effects were noticed in the B-ALL PDX model administrated with anlotinib. All these observed findings inform that clinical treatment of patients with RR B-ALL with anlotinib is probably feasible regarding its attractive preclinical anti-B-ALL effects and tolerable adverse effects.

In concert with prior published series, we observed that anlotinib exerted its cytotoxicity against Ph^- and Ph^+ B-ALL preclinical models potentially through interference with the proangiogenic functional targets, including VEGFR2, PDGFR-beta, and FGFR3. The PI3K/AKT/mTOR signaling cascade is a classical prosurvival pathway and plays an essential role in promoting cell proliferation and survival in normal circumstances. Aberrant activation of PI3K and its downstream AKT/mTOR signaling is often observed in a variety of malignant diseases, including B-ALL [42]. Aberration of the PI3K/AKT/mTOR pathway is closely associated with chemoresistance and inferior prognosis in pediatric and adult B-ALL patients [43]. Accordingly, blockade of the activity of the PI3K/AKT/mTOR pathway has been widely evaluated in B-ALL cellular models with encouraging results, thus prompting several small molecular inhibitors targeting the PI3K/AKT cascade entering clinical evaluation [44]. Of interest, the PI3K/AKT/mTOR cascade resides in the convergence of the three important proangiogenic signaling pathways [45,46], suggesting that anlotinib induced proangiogenic signal reduction might result in a perturbation of the function of the PI3K/AKT/mTOR pathway. Not surprisingly, in the present study, exposure of Ph^- and Ph^+ B-ALL cells to anlotinib indeed decreased the phosphorylation levels of PI3K and its downstream componenets AKT and mTOR.

Conclusion

This study found that patients with RR B-ALL showed an elevated proangiogenic activity and an increased activity of the PI3K/AKT/

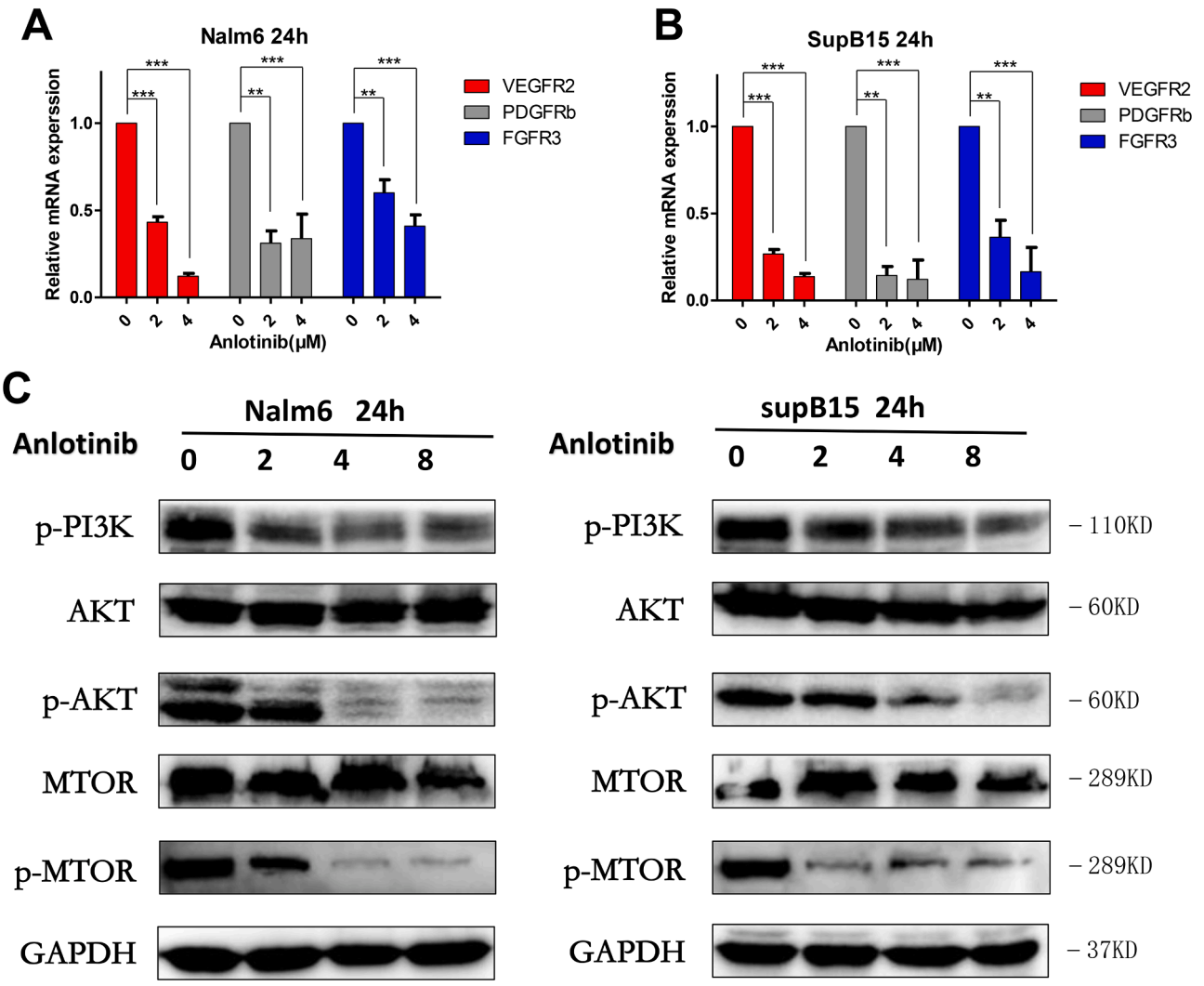

Fig. 4. Anlotinib decreases the levels of key proangiogenic mediators and blunts the activity of PI3K/AKT/mTOR pathway in Ph^- and Ph^+ B-ALL cells. Nalm6 and SupB15 cells were treated with or without anlotinib for 24 h. (A) & (B) Real-time quantitative PCR analysis of mRNA levels of VEGFR2, PDGFR-beta, and FGFR3. (C) Western blot analysis of the expression of p-PI3K, p-AKT, AKT, mTOR, and p-mTOR.

mTOR pathway, a pivotal downstream cascade of angiogenesis. Anlotinib, an inhibitor of VEGFR, PDGFR, and FGFR which are the three main proangiogenic factors, was potent to induce cell viability reduction, promote cell apoptosis, and accumulate cell cycle at G2/M phase in Ph^- and Ph^+ B-ALL cellular models. *In vivo* experiments, oral administration with anlotinib significantly abrogated the leukemia burden and prolonged the survival duration in a Ph^+ B-ALL PDX model. Mechanistically, downregulation of the expression levels of VEGFR2, PDGFR-beta, and FGFR3 was associated with the cytotoxicity of anlotinib against Ph^- and Ph^+ B-ALL. Furthermore, the PI3K/AKT/mTOR pathway was significantly inactiviated by anlotinib, indicating that perturbation of this pathway was a potential mechanism of action of anlotinib in the management of Ph^- and Ph^+ B-ALL. Overall, our preclinical results provide a promising rational therapeutic option for the treatment of Ph^- and Ph^+ B-ALL but need further confirmatory investigations in clinical trials.

Funding

This work was supported by the National Natural Science Foundation of China (81770126, 81770161, and 81800163), The the Natural Science Foundation of Fujian Province (2019J0105, 2019J01581), Foundation of health and family planning Commission of in Fujian Province of China (2017-2-99, 2018-2-63) and Beijing Medical and Health Foundation (F3100C).

Author contribution statement

Conception and design: QLC, YZ, MMD, BX. Development of methodology: QLC, QL, YLJ, JWY, QWC. Analysis and interpretation of data: QLC, QL, YLJ, QWC, GSC, YZ, MMD, BX. Writing, review, and/or revision of the manuscript: QLC, MMD, BX. Study supervision: YZ, MMD, BX. All authors have accepted responsibility for the entire content of this manuscript and approved its submission.

Ethics approval and consent to participate

All animal studies were performed following protocols approved by Xiamen University Animal Care and Use Committee (XMULAC20170065).

Human and animal rights

The B-ALL primary sample used in the PDX model was obtained from Department of Hematology, the First Affiliated Hospital of Xiamen University with the informed consent for research purposes only from

the B-ALL patient. This animal study was performed in accordance with the Declaration of Helsinki and approved by Ethics Review Board of First Affiliated Hospital of Xiamen University.

Availability of data and materials

All relevant data and materials have been involved in the article. Further inquiries can be directed to the corresponding authors.

Declaration of Competing Interest

All authors declare no conflict of interest.

Acknowledgment

Declared None.

Supplementary materials

Supplementary material associated with this article can be found, in the online version, at doi:10.1016/j.tranon.2022.101516.

References

[1] T. Terwilliger, M. Abdul-Hay, Acute lymphoblastic leukemia: a comprehensive review and 2017 update, Blood Cancer J. 7 (2017) e577, https://doi.org/10.1038/bcj.2017.53.
[2] L. Komorowski, K. Fidyt, E. Patkowska, M. Firczuk, Philadelphia chromosome-positive leukemia in the lymphoid lineage-similarities and differences with the myeloid lineage and specific vulnerabilities, Int. J. Mol. Sci. 21 (2020), https://doi.org/10.3390/ijms21165776.
[3] M.A. Smith, et al., Outcomes for children and adolescents with cancer: challenges for the twenty-first century, J. Clin. Oncol. 28 (2010) 2625–2634, https://doi.org/10.1200/JCO.2009.27.0421.
[4] D. Bhojwani, C.H. Pui, Relapsed childhood acute lymphoblastic leukaemia, Lancet Oncol. 14 (2013) e205–e217, https://doi.org/10.1016/S1470-2045(12)70580-6.
[5] M.B. Geyer, et al., Overall survival among older US adults with ALL remains low despite modest improvement since 1980: SEER analysis, Blood 129 (2017) 1878–1881, https://doi.org/10.1182/blood-2016-11-749507.
[6] S.P. Hunger, C.G. Mullighan, Redefining ALL classification: toward detecting high-risk ALL and implementing precision medicine, Blood 125 (2015) 3977–3987, https://doi.org/10.1182/blood-2015-02-580043.
[7] K. Fousek, et al., CAR T-cells that target acute B-lineage leukemia irrespective of CD19 expression, Leukemia 35 (2021) 75–89, https://doi.org/10.1038/s41375-020-0792-2.
[8] H. Kantarjian, et al., Blinatumomab versus chemotherapy for advanced acute lymphoblastic leukemia, N. Engl. J. Med. 376 (2017) 836–847, https://doi.org/10.1056/NEJMoa1609783.
[9] K. Wudhikarn, et al., Interventions and outcomes of adult patients with B-ALL progressing after CD19 chimeric antigen receptor T-cell therapy, Blood 138 (2021) 531–543, https://doi.org/10.1182/blood.2020009515.
[10] M. De Palma, D. Biziato, T.V. Petrova, Microenvironmental regulation of tumour angiogenesis, Nat. Rev. Cancer 17 (2017) 457–474, https://doi.org/10.1038/nrc.2017.51.
[11] D. Passaro, et al., Increased vascular permeability in the bone marrow microenvironment contributes to disease progression and drug response in acute myeloid leukemia, Cancer Cell 32 (2017) 324–341, https://doi.org/10.1016/j.ccell.2017.08.001, e326.
[12] S. Kazerounian, J. Lawler, Integration of pro- and anti-angiogenic signals by endothelial cells, J. Cell. Commun. Signal. 12 (2018) 171–179, https://doi.org/10.1007/s12079-017-0433-3.
[13] M. Simons, E. Gordon, L. Claesson-Welsh, Mechanisms and regulation of endothelial VEGF receptor signalling, Nat. Rev. Mol. Cell Biol. 17 (2016) 611–625, https://doi.org/10.1038/nrm.2016.87.
[14] S. Qin, et al., Recent advances on anti-angiogenesis receptor tyrosine kinase inhibitors in cancer therapy, J. Hematol. Oncol. 12 (2019) 27, https://doi.org/10.1186/s13045-019-0718-5.
[15] G.C. Jayson, R. Kerbel, L.M. Ellis, A.L. Harris, Antiangiogenic therapy in oncology: current status and future directions, Lancet 388 (2016) 518–529, https://doi.org/10.1016/S0140-6736(15)01088-0.
[16] T. Annese, R. Tamma, S. Ruggieri, D. Ribatti, Angiogenesis in pancreatic cancer: pre-clinical and clinical studies, Cancers (Basel) 11 (2019), https://doi.org/10.3390/cancers11030381.
[17] S. Faderl, et al., Angiogenic factors may have a different prognostic role in adult acute lymphoblastic leukemia, Blood 106 (2005) 4303–4307, https://doi.org/10.1182/blood-2005-03-1010.
[18] E. Diffner, et al., Expression of VEGF and VEGF receptors in childhood precursor B-cell acute lymphoblastic leukemia evaluated by immunohistochemistry, J. Pediatr. Hematol. Oncol. 31 (2009) 696–701, https://doi.org/10.1097/MPH.0b013e3181b258df.
[19] M. Deng, et al., Apatinib exhibits anti-leukemia activity in preclinical models of acute lymphoblastic leukemia, J. Transl. Med. 16 (2018) 47, https://doi.org/10.1186/s12967-018-1421-y.
[20] G. Shen, et al., Anlotinib: a novel multi-targeting tyrosine kinase inhibitor in clinical development, J. Hematol. Oncol. 11 (2018) 120, https://doi.org/10.1186/s13045-018-0664-7.
[21] K. Zhang, et al., Efficacy and safety of anlotinib in advanced non-small cell lung cancer: a real-world study, Cancer Manag. Res. 12 (2020) 3409–3417, https://doi.org/10.2147/CMAR.S246000.
[22] B. Han, et al., Anlotinib as a third-line therapy in patients with refractory advanced non-small-cell lung cancer: a multicentre, randomised phase II trial (ALTER0302), Br. J. Cancer 118 (2018) 654–661, https://doi.org/10.1038/bjc.2017.478.
[23] Y.Y. Syed, Anlotinib: first global approval, Drugs 78 (2018) 1057–1062, https://doi.org/10.1007/s40265-018-0939-x.
[24] Y. Chi, et al., Safety and efficacy of anlotinib, a multikinase angiogenesis inhibitor, in patients with refractory metastatic soft-tissue sarcoma, Clin. Cancer Res. 24 (2018) 5233–5238, https://doi.org/10.1158/1078-0432.CCR-17-3766.
[25] Y. Sun, et al., Safety, pharmacokinetics, and antitumor properties of anlotinib, an oral multi-target tyrosine kinase inhibitor, in patients with advanced refractory solid tumors, J. Hematol. Oncol. 9 (2016) 105, https://doi.org/10.1186/s13045-016-0332-8.
[26] J. Wang, D.X. Wu, L. Meng, G. Ji, Anlotinib combined with SOX regimen (S1 (tegafur, gimeracil and oteracil porassium capsules) + oxaliplatin) in treating stage IV gastric cancer: study protocol for a single-armed and single-centred clinical trial, BMJ Open 10 (2020), e034685, https://doi.org/10.1136/bmjopen-2019-034685.
[27] L. Gautier, L. Cope, B.M. Bolstad, R.A. Irizarry, affy–analysis of Affymetrix GeneChip data at the probe level, Bioinformatics 20 (2004) 307–315, https://doi.org/10.1093/bioinformatics/btg405.
[28] I. Diboun, L. Wernisch, C.A. Orengo, M. Koltzenburg, Microarray analysis after RNA amplification can detect pronounced differences in gene expression using limma, BMC Genomics 7 (2006) 252, https://doi.org/10.1186/1471-2164-7-252.
[29] G. Dennis Jr., et al., DAVID: database for annotation, visualization, and integrated discovery, Genome Biol. 4 (2003). P3.
[30] E.Y. Chen, et al., Expression2Kinases: mRNA profiling linked to multiple upstream regulatory layers, Bioinformatics 28 (2012) 105–111, https://doi.org/10.1093/bioinformatics/btr625.
[31] J. Chen, et al., Anlotinib suppresses MLL-rearranged acute myeloid leukemia cell growth by inhibiting SETD1A/AKT-mediated DNA damage response, Am. J. Transl. Res. 13 (2021) 1494–1504.
[32] M. Kanehisa, Y. Sato, M. Kawashima, M. Furumichi, M. Tanabe, KEGG as a reference resource for gene and protein annotation, Nucleic. Acids. Res. 44 (2016) D457–D462, https://doi.org/10.1093/nar/gkv1070.
[33] P. Sujobert, et al., Essential role for the p110delta isoform in phosphoinositide 3-kinase activation and cell proliferation in acute myeloid leukemia, Blood 106 (2005) 1063–1066, https://doi.org/10.1182/blood-2004-08-3225.
[34] J. Potratz, et al., Receptor tyrosine kinase gene expression profiles of Ewing sarcomas reveal ROR1 as a potential therapeutic target in metastatic disease, Mol Oncol 10 (2016) 677–692, https://doi.org/10.1016/j.molonc.2015.12.009.
[35] Z. Du, C.M. Lovly, Mechanisms of receptor tyrosine kinase activation in cancer, Mol. Cancer 17 (2018) 58, https://doi.org/10.1186/s12943-018-0782-4.
[36] Y. Ling, Q. Xie, Z. Zhang, H. Zhang, Protein kinase inhibitors for acute leukemia, Biomark. Res. 6 (2018) 8, https://doi.org/10.1186/s40364-018-0123-1.
[37] R.A. Chougule, K. Shah, S.A. Moharram, J. Vallon-Christersson, J.U. Kazi, Glucocorticoid-resistant B cell acute lymphoblastic leukemia displays receptor tyrosine kinase activation, NPJ. Genom. Med. 4 (2019) 7, https://doi.org/10.1038/s41525-019-0082-y.
[38] F. Song, et al., Anlotinib suppresses tumor progression via blocking the VEGFR2/PI3K/AKT cascade in intrahepatic cholangiocarcinoma, Cell Death. Dis. 11 (2020) 573, https://doi.org/10.1038/s41419-020-02749-7.
[39] J. Bruix, et al., Adjuvant sorafenib for hepatocellular carcinoma after resection or ablation (STORM): a phase 3, randomised, double-blind, placebo-controlled trial, Lancet Oncol. 16 (2015) 1344–1354, https://doi.org/10.1016/S1470-2045(15)00198-9.
[40] Y. Itatani, K. Kawada, T. Yamamoto, Y. Sakai, Resistance to anti-angiogenic therapy in cancer-alterations to anti-VEGF pathway, Int. J. Mol. Sci. 19 (2018), https://doi.org/10.3390/ijms19041232.
[41] K. Hosaka, et al., Dual roles of endothelial FGF-2-FGFR1-PDGF-BB and perivascular FGF-2-FGFR2-PDGFRbeta signaling pathways in tumor vascular remodeling, Cell. Discov. 4 (2018) 3, https://doi.org/10.1038/s41421-017-0002-1.
[42] F. Janku, T.A. Yap, F. Meric-Bernstam, Targeting the PI3K pathway in cancer: are we making headway? Nat. Rev. Clin. Oncol. 15 (2018) 273–291, https://doi.org/10.1038/nrclinonc.2018.28.
[43] L.M. Neri, et al., Targeting the PI3K/Akt/mTOR signaling pathway in B-precursor acute lymphoblastic leukemia and its therapeutic potential, Leukemia 28 (2014) 739–748, https://doi.org/10.1038/leu.2013.226.
[44] L. Fransecky, L.H. Mochmann, C.D. Baldus, Outlook on PI3K/AKT/mTOR inhibition in acute leukemia, Mol. Cell. Ther. 3 (2015) 2, https://doi.org/10.1186/s40591-015-0040-8.
[45] M. Deng, et al., Apatinib exhibits cytotoxicity toward leukemia cells by targeting VEGFR2-mediated prosurvival signaling and angiogenesis, Exp. Cell. Res. 390 (2020), 111934, https://doi.org/10.1016/j.yexcr.2020.111934.
[46] H. Zhang, et al., PDGFRs are critical for PI3K/Akt activation and negatively regulated by mTOR, J. Clin. Invest. 117 (2007) 730–738, https://doi.org/10.1172/JCI28984.